f–d transitions and self-trapped excitons in CsCdBr$_3$: Eu^{2+}

f–d transitions and self-trapped excitons in CsCdBr$_3$: Eu^{2+}

S García-Revilla and R Valiente

Departamento de Física Aplicada, Facultad de Ciencias, Universidad de Cantabria, 39005, Santander, Spain

Abstract

Single crystals of CsCdBr$_3$ doped with Eu^{2+} at different concentrations were grown by the Bridgman technique and studied by polarized variable-temperature optical absorption and luminescence spectroscopy for different excitation wavelengths. Absorption bands of different natures were assigned in terms of concentration behaviour and temperature dependent photoluminescence. The low-energy structured band was due to f $\rightarrow$ d transitions within the Eu^{2+} electronic configuration. The proximity of the high-energy d levels to the conduction band induces self-ionization of Eu^{2+}. The high-energy absorption bands were assigned to self-trapped excitons.

Dedicated to Professor Hans U Güdel on the occasion of his 65th birthday.

1. Introduction

Rare-earth ions are present in solids as trivalent (RE^{3+}) or divalent (RE^{2+}) states. The shielding character of the 4f orbitals by the filled 5s^2 and 5p^6 orbitals determines the weak interaction with the neighbouring ions. This explains the small influence of the host lattice and the sharp lines observed in spectra based on f–f transitions. Thus, the Dieke diagram predicts, independently of the host lattice, most of the spectroscopic properties of the intraconfigurational f–f transitions. The Judd–Ofelt theory calculates transition probabilities, and the non-radiative multiphonon relaxation processes are anticipated by the gap's law.

However, f–d transitions are not well understood, partly because in trivalent ions they generally lie in the ultraviolet region (6.2 eV above the ground term) and therefore are experimentally less accessible. However, in the past few years, the study of the parity allowed 4f $\rightarrow$ 5d transitions of the divalent lanthanides has increased because their excited states are relatively low in energy and easily accessible. Sm^{2+}, Eu^{2+}, Tm^{2+} and Yb^{2+} ions in inorganic solids are easy to stabilize. Eu^{2+} is the most stable divalent lanthanide due to its half-filled (4f^7) valence shell. All the other RE^{2+} ions are obtained by irradiation [1, 2].

In contrast to 4f $\rightarrow$ 4f transitions, absorption and emission bands corresponding to the 4f $\leftrightarrow$ 5d transitions are very sensitive to the crystal-field environment of the host lattice

site. Therefore, f–d transitions are characterized by broad bands and the relative position of the excited levels depends on distinct factors such as crystal field strength, covalence or coordination number. Most of the increasing interest in RE^{2+} is due to the application of these materials as phosphors for lamps, displays or tunable lasers in the vacuum UV, where the transition from the excited state configuration $4f^{n-1}5d^1$ to the ground state configuration $4f^n$ plays an important role.

McClure and Kiss, and Loh, studied for the first time the general features of the absorption spectra of RE^{2+}-doped CaF_2 [1, 2]. Rubio and co-workers studied the spectroscopic properties of Eu^{2+}-doped alkali halides [3]. Irradiated Eu^{2+}-doped CaF_2 or alkali halides made difficult a proper correlation between structure and electronic properties because of the presence of charge compensation, defects or vacancies. Eu^{2+}-doped inorganic compounds are used as phosphor imaging plates for diagnostic radiography. In particular, Eu^{2+}-doped BaFBr is one of the best commercially used x-ray phosphors up to now. The erasable x-ray imaging plates have developed x-ray detection in medicine, physics and biology. The advantage of this system is its dynamical range and the processing speed. Several models have been proposed for the storage process. However, although the photo-stimulated luminescence (PSL) is expected to be due to the presence of some centres with a high luminescence yield under stimulation, its fundamental mechanism must still be clarified [4]. This fact has increased the number of studies on Eu^{2+} in many different lattices in order to correlate the PSL mechanism with structural properties (aggregation) [5] and to improve the efficiency of such a mechanism. Recently, Dorenbos has carried out an extensive review work on the spectroscopic data of Eu^{2+}-doped inorganic compounds [6, 7].

Throughout this paper, we will try to correlate the optical properties with the electronic and crystal structure. We chose $CsCdBr_3$ as a host lattice because the Eu^{2+} local arrangement is well established. Eu^{2+} dopant ions substitute the divalent cation site and therefore charge compensation is not required. Moreover, detailed information can be obtained from the polarized absorption due to its essentially one-dimensional structure. We perform a detailed investigation of the polarized absorption, photoluminescence (PL) and excitation spectra of Eu^{2+}-doped $CsCdBr_3$ as a function of temperature and concentration.

2. Experimental details

Single crystals of $CsCdBr_3$: Eu^{2+} were grown from the melt by the vertical Bridgman technique using stoichiometric amounts of CsBr (Aldrich 99.9%), $CdBr_2$ (Aldrich 99.999%) and $EuBr_2$ (Aldrich 99.99%). Eu^{2+} nominal concentrations of 1%, 0.1% and 0.01% were used. In addition, some small chips of Cd metal were added to the quartz ampoule in order to avoid the formation of Eu^{3+}. At all stages of growth and handling, the materials were kept and handled in an inert atmosphere of either vacuum, He or Ar, to prevent the adsorption of water. The grown crystals are yellow–greenish, of excellent optical quality.

$CsCdBr_3$ crystal structure belongs to the $P6_3/mmc$ space group. It consists of linear chains of face-sharing $[CdBr_6]^{4-}$ octahedra arranged along the crystallographic c axis. Because the distance between the Cd^{2+} ions along a chain (3.361 Å) is much less than the separation between chains (7.675 Å), this compound possesses a distinct one-dimensional character [8]. Eu^{2+} occupies the Cd^{2+} site in the $CsCdBr_3$ host lattice. The site symmetry is almost octahedral with slight trigonal distortion along the axis of the chain.

Polarized absorption spectra were measured with a Lambda 9 UV–vis–NIR Perkin-Elmer spectrophotometer equipped with Glan-Taylor polarizing prisms. The single crystals were selected and oriented using a polarizing microscope.

For PL and excitation spectroscopy, a Jobin-Yvon Fluoromax-2 fluorometer equipped with a 150 W Xe lamp as excitation source was used. Suitable interferential and cutting filters were
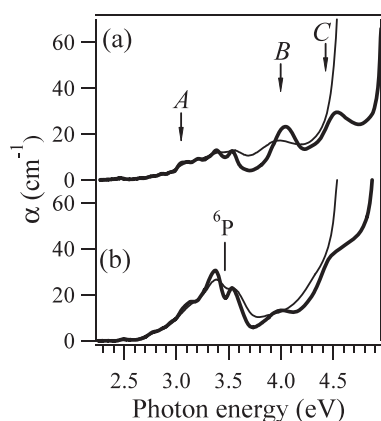
Figure 1. Room-temperature (thin line) and 10 K (thick line) polarized survey absorption spectra of a CsCdBr$_3$: 0.1% Eu^{2+} single crystal with $\mathbf{E} \perp \mathbf{c}$ (a) and $\mathbf{E} \parallel \mathbf{c}$ (b). The labels of the absorption bands are used in the text. The arrows correspond to the excitation energies used in the PL measurements. The energetic position of the Eu^{2+} ^{6}P excited state within the 4f^7 electronic configuration is indicated.
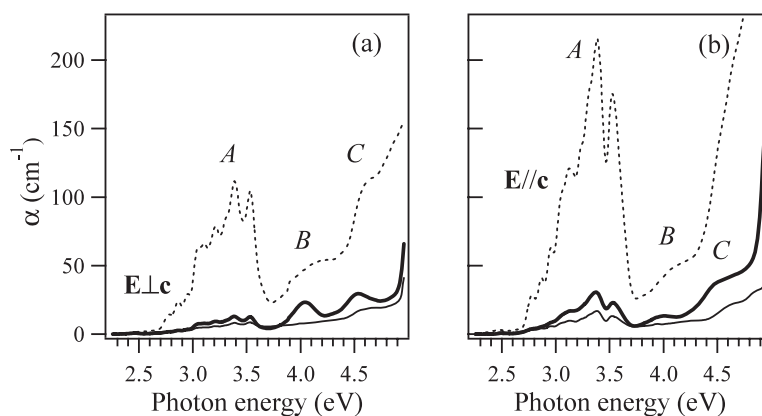

Figure 2. 10 K polarized survey absorption spectra with $\mathbf{E} \perp \mathbf{c}$ (a) and $\mathbf{E} \parallel \mathbf{c}$ (b) of CsCdBr$_3$ single crystals doped with 0.01% (thin line), 0.1% (thick line) and 1% Eu^{2+} (broken line).

employed to avoid the straight light. Sample cooling was achieved using a closed-cycle He cryostat Scientific Instrument 202 and an APD-K temperature controller in the 10–300 K range for emission and absorption experiments.

All excitation and PL spectra were corrected for the instrumental response of the system.

3. Results

Figure 1 shows the room-temperature and 10 K polarized optical absorption spectra of a CsCdBr$_3$: 0.1% Eu^{2+} single crystal with $\mathbf{E} \perp \mathbf{c}$ and $\mathbf{E} \parallel \mathbf{c}$. The **c**-direction corresponds to the hexagonal optical axis of the CsCdBr$_3$ crystals. The absorption spectra consist of three bands. The lower-energy band presents fine structure and extends from 2.42 to 3.72 eV (band A). Additionally, another two structureless bands at 4.04 eV (B) and 4.54 eV (C) show an opposite polarization behaviour compared to the lower energy one. Figure 2 compares the 10 K
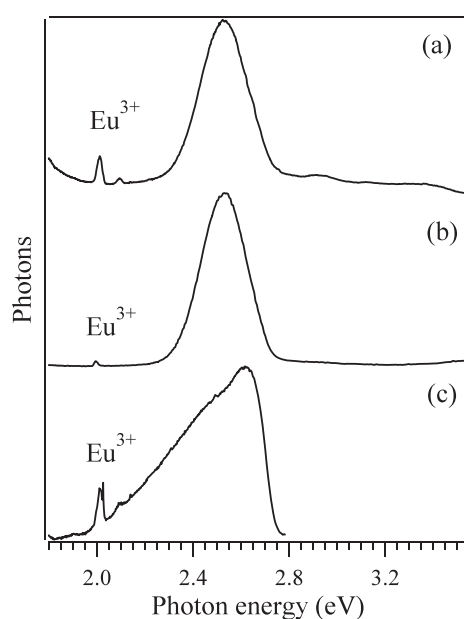
Figure 3. 10 K unpolarized PL spectra of CsCdBr$_3$: 0.1% Eu^{2+} exciting at 4.44 (a), 4.00 (b) and 3.05 eV (c).

absorption spectra with $\mathbf{E} \perp \mathbf{c}$ and $\mathbf{E} \parallel \mathbf{c}$ for different Eu^{2+} concentrations. It is remarkable that the absorption intensity of the low-energy band grows with Eu^{2+} concentration, while the other two bands do not have the same behaviour.

10 K unpolarized PL spectra of CsCdBr$_3$: 0.1% Eu^{2+} after excitation at 4.44 eV (a), 4.00 eV (b) and 3.05 eV (c) are shown in figure 3. The excitation energies are shown as arrows in figure 1(a). In the first two cases, the PL spectra consist of an unstructured strong broad symmetric band peaking at 2.53 eV, whereas the excitation into the lower energy band induces a completely different asymmetric PL band peaking at 2.63 eV. Similar spectra were observed for the other Eu^{2+} concentrations. Sharp peaks at 2.01 and 2.09 eV are assigned to the $^5D_0 \rightarrow {}^7F_2, {}^7F_1$ transitions of Eu^{3+} traces. The temperature dependence of the three PL bands of CsCdBr$_3$: Eu^{2+} has been determined in the 10–300 K range for different excitation energies (figure 4). The PL intensities were corrected for the temperature dependence of the absorption cross-section at the excitation energies. Again, the PL band at 3.05 eV excitation energy gives rise to a distinct behaviour compared to the PL after excitation at 4.00 and 4.44 eV. This is important evidence in order to assign the different origins of the absorption bands, as we shall see.

The corresponding excitation spectrum (figure 5) presents two prominent broad bands corresponding to the higher energy absorption bands observed at 10 K (figure 1). The relative intensities of the high- and low-energy bands in the excitation spectrum are not comparable with those observed in the absorption spectra.

4. Analysis and discussion

In the ground state of Eu^{2+} ions there are seven 4f electrons, which, according to Hund's rules, give rise to the ground state $^8S_{7/2}$. However, the lowest-lying excited states may be
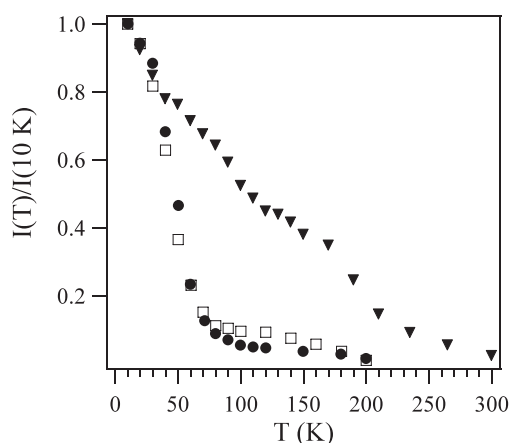
Figure 4. Temperature dependence of the normalized integrated Eu^{2+} PL intensities in CsCdBr$_3$: 0.1% Eu^{2+} after exciting at 4.44 eV (squares), 4.00 eV (dots) and 3.05 eV (triangles). They are corrected for the temperature dependence of the absorption cross section at the excitation energies.
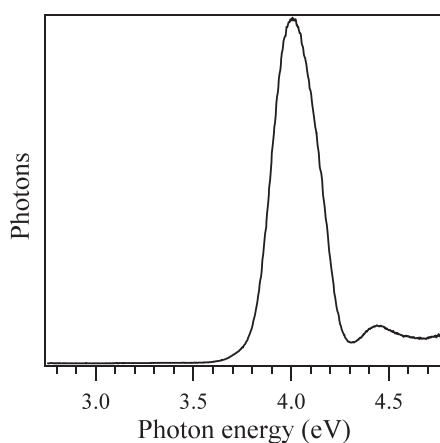

Figure 5. 10 K excitation spectrum of CsCdBr$_3$: 0.1% Eu^{2+} monitoring the Eu^{2+} PL at 2.53 eV.

formed either by states within the 4f^7 configuration such as ^{6}P, ^{6}I, ^{6}D, or from states within the 4f^{6}5d^1 configuration. In an octahedral symmetry, the degenerated 5d levels corresponding to the former excited configuration are shifted and split into t$_{2g}$ and e$_g$ components. Therefore, the absorption spectrum of Eu^{2+} in a crystal typically shows two broad absorption bands corresponding to the 4f^7(^{8}S$_{7/2}$) $\rightarrow$ 4f^{6}5d^1(t$_{2g}$) and 4f^7(^{8}S$_{7/2}$) $\rightarrow$ 4f^{6}5d^1(e$_g$) transitions. The separation between them is the well known 10Dq splitting, that reflects the crystal field strength.

In figure 1 the low-temperature polarized absorption spectra of CsCdBr$_3$: 0.1% Eu^{2+} are well resolved. The low-energy band A, extending from 2.42 to 3.72 eV, was previously observed by Pellé *et al* in the unpolarized absorption spectrum of this host lattice doped with 0.2% Eu^{2+} [9]. This band was assigned to transitions from the Eu^{2+} ^{8}S$_{7/2}$ ground state to the T$_{2g}$ excited state of the 4f^{6}5d^1 electronic configuration. Its characteristic 'staircase' structure was originally explained by the splitting of the ground state of the 4f^6 core and the 5d electron assuming a weak or null Coulomb interaction, i.e., by transitions from the ^{8}S$_{7/2}$ to the seven
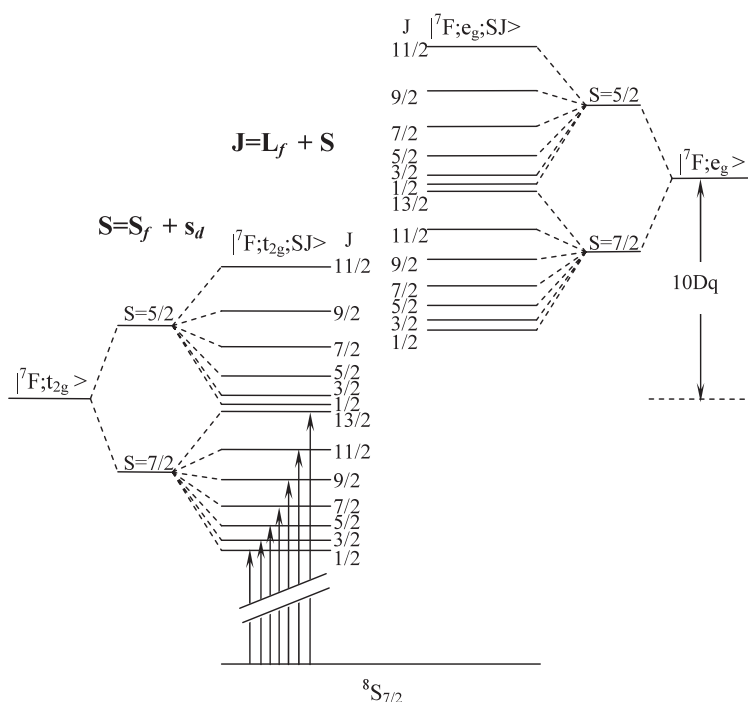
Figure 6. Schematic diagram of the Eu^{2+} energetic levels within the $4f^65d$ configuration in an octahedral crystal field following the model proposed by Duan *et al* [11, 12]. S_f and L_f are the total spin and orbital quantum numbers of the f electrons and s_d is the spin of the d electron.

^7F_J multiplets ($J = 0$–6) of the excited $4f^6(^7F_J)5d^1(t_{2g})$ configuration [7]. The splitting of the J-multiplets is the result of the Coulomb interaction between the six 4f electrons and their spin–orbit coupling. The similarity between peak energy differences of this 'staircase' structure and those of the $^7F_0$–$^7F_6$ Eu^{3+} multiplets supported this idea. However, previous calculations have shown that Coulomb interaction between 4f and 5d electrons cannot be neglected [10]. Two complementary models can explain the structure of the A absorption band depending on the relative magnitudes of the former interaction (H′(4f–5d)) and the 4f spin–orbit effect (H_{SO}(4f)) [11–13]. Figures 6 and 7 show the energy level schemes obtained using both perturbative models for Eu^{2+} in an octahedral crystal field. Although the actual symmetry of Eu^{2+} doped $CsCdBr_3$ is D_{3d}, it is possible to use the octahedral approximation since the trigonal distortion is small. The energetic diagram shown in figure 6 is valid when the effect of H′(4f–5d) is larger than H_{SO} (4f) [11, 12]. In this case, the 'staircase' band structure corresponds to the f–d absorption ($\Delta S = 0$) from the $^8S_{7/2}$ ground state to the high-spin levels ($S = 7/2$) associated with $|^7F; t_{2g}; ^8F_J\rangle$ and $|^7F; e_g; ^8F_J\rangle$ states ($J = 13/2, 11/2, \ldots, 1/2$). Transitions from $^8S_{7/2}$ to low-spin levels ($S = 5/2$) are spin forbidden. However, if H_{SO}(4f) > H′(4f–5d) the A absorption band can be understood within the second model [13] through the arrows plotted in figure 7. Note that the $^8S_{7/2} \rightarrow |^7F_J; t_{2g}; S = 7/2\rangle$ are spin allowed.

Moreover, a careful analysis of the lower-energy absorption band of Eu^{2+} compounds requires taking into account that it overlaps with the ^6P_J terms of the $4f^7$ Eu^{2+} electronic configuration [14]. Downer *et al* determined the transition energies of the $^8S_{7/2} \rightarrow {}^6P_J, {}^6I_J$, ^6D_J intraconfigurational transitions of Eu^{2+}-doped CaF_2 and SrF_2 by two-photon absorption spectroscopy [15]. The excited state interaction of the $4f^7$ and $4f^65d^1$ configurations gives
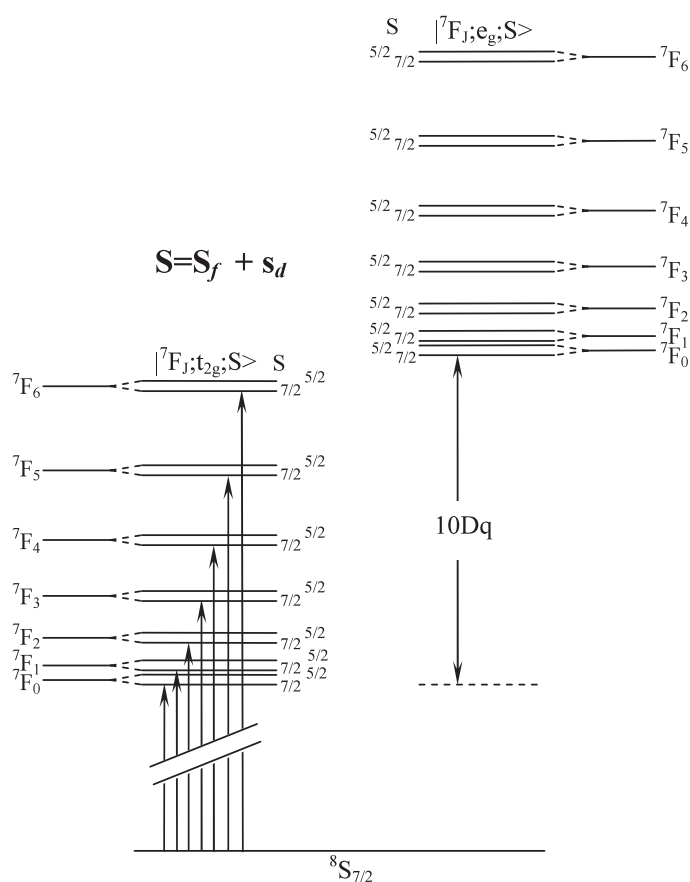
Figure 7. Schematic diagram of the Eu^{2+} energetic levels within the 4f^{6}5d configuration in an octahedral crystal field following the model proposed by Güdel [13]. S_f is the total spin of the f electrons and s_d is the spin of the d electron.

rise to the Fano antiresonance previously observed by Pellé *et al* [9]. The ^{6}P energy level is indicated in figure 1.

The assignment of the B and C high-energy bands (figure 1) is more intricate. In the absorption spectrum reported by Pellé *et al* only a high-energy band centred at 4.23 eV was present as a shoulder within the absorption edge. This band was associated with the transition from the ^{8}S$_{7/2}$ to the corresponding e$_g$ levels of the 4f^{6}5d^1 configuration. From the separation of their two absorption bands the authors extracted a $10Dq$ value of 0.93 eV. At first sight, this crystal-field splitting for the 5d electron is very small considering that values at about 0.9 eV are usual in 3d transition metal ions. It is well known that $10Dq(5d) \geqslant 10Dq(4d) \gg 10Dq(3d)$. The fact that $10Dq$ is much bigger than the spin pairing energy makes it possible that 4d and 5d ions present low-spin configurations. Systems based on 4d and 5d ions have $10Dq$ values higher than 2.48 eV. By way of example, Rh^{3+} in fluorides shows $10Dq \approx 2.8$ eV, whereas Mo^{3+} in chlorides $10Dq \approx 2.73$ eV [16]. From the analysis of the absorption spectrum of CaF$_2$: Eu^{2+}, a $10Dq \approx 2.11$ eV value was obtained [2]. Taking into account the difference of ionic radii and that the symmetry of Eu^{2+} in this lattice is cubic and not octahedral, we can estimate a $10Dq$ value of about 1.61 eV. Crystal field theory predicts that $10Dq$ parameter

varies with Eu^{2+}–ligand distance, R, as R^{-5}. On the other hand, assuming equal distances, the ligand field in octahedral coordination is reduced compared to eightfold cubic symmetry ($10Dq(\text{cub}) = 8/3 \times 10Dq(O_h)$) [17]. Additionally, in Eu^{2+} compounds, Dorenbos has found that $10Dq$ changes as βR^{-2} [18], where β depends on the coordination polyhedron. According to the available $10Dq$ values in octahedral coordination, a $10Dq \approx 1.49$ eV value for Eu^{2+}-doped $CsCdBr_3$ is estimated [18]. Since the $^8S_{7/2} \to 4f^65d$ (t_{2g}) is about 3.34 eV, one would expect that the $^8S_{7/2} \to 4f^65d$ (e_g) transition be placed around 4.84 eV. Taking into account that the energy gap of $CsCdBr_3$ is $E_g \sim 4.8$–4.9 eV [19], the $^8S_{7/2} \to 4f^65d$ (e_g) transition would be close to or even inside the conduction band. This fact is relevant for identifying the two high-energy bands which present a different polarization and concentration dependence of their absorption intensities (figure 2).

In order to clarify the origin of the bands B and C peaking at 4.04 and 4.54 eV, respectively, we have obtained the 10 K PL spectra exciting in the different absorption bands (figure 1) as well as their temperature dependence (figures 3 and 4). Excitation in the A absorption band at 3.05 eV leads to an asymmetric PL band peaking at 2.63 eV with a long tail up to 1.98 eV (see figure 3). We associate this band with the 'normal' Eu^{2+} emission, corresponding to the transition from the low-energy level of the $4f^65d^1$ (t_{2g}) electronic configuration to the ground state $^8S_{7/2}$. The asymmetric shape of the PL band has been observed previously in other systems like $LaBr_3$: Eu^{2+} [20]. The integrated intensity of this PL band shows smooth temperature dependence (figure 4). However, excitation into bands B and C at 4.00 and 4.44 eV, respectively, presents analogous PL. In both cases, the PL spectrum contains a broad Gaussian band centred at 2.53 eV (figure 3), by contrast to that observed around 3.05 eV excitation. This result unambiguously indicates the distinct origin of these absorption bands. Moreover, excitation in both high-energy bands presents an unusually large Stokes shift and an abrupt change of the PL intensity upon increasing temperature (figure 4). On the other hand, the excitation spectrum reveals that the excitation into the two high-energy absorption bands is more efficient for inducing green PL (figure 5). These results indicate the distinct origin of bands B and C peaking at 4.04 and 4.54 eV and the structured band at 3.35 eV. Therefore, it is unlikely that the B and C bands could be associated with transitions from the $^8S_{7/2}$ to the e_g components of the $4f^65d^1$ configuration.

Heber *et al* have identified in the excitation spectrum of pure $CsCdBr_3$ two types of excitons, lattice and localized in defects or impurities [21]. Two bands centred at 5.17 eV and another structured band between 4.22 and 4.96 eV are the fingerprints of the two excitons. These two bands do not correspond with those found in our $CsCdBr_3$: Eu^{2+} compounds discarding this origin.

In inorganic materials doped with Eu^{2+}, the 5d levels are close to or inside the conduction band. Then, the 5d orbital wavefunction can mix with the wavefunction of the conduction band. So, it is possible that after excitation of one 4f electron to the 5d orbital, self-ionization of Eu^{2+} ($Eu^{2+} \to e^- + Eu^{3+}$, e^-–hole) takes place. The free electron delocalized in the conduction band can be trapped near the Eu^{3+} (hole) giving rise to localized levels, self-trapped exciton (STE) states. The recombination of the e^-–hole pair can produce non-radiative processes or luminescence with a large Stokes shift. This emission was denominated 'anomalous' by McClure [22] and Dorenbos [7]. The large Stokes shift observed can be explained on the basis of the distortion induced in the excited state with respect to the ground state geometry of the STE. This effect is a consequence of the different radii between Eu^{3+} and Eu^{2+} (19 pm) [7]. After creation of STE, Br^- ligands collapse towards Eu^{3+}.

Therefore, a possible interpretation of the results obtained in $CsCdBr_3$: Eu^{2+} is that after excitation at 4.00 and 4.44 eV an impurity STE is created. This would account for the Stokes shift and the temperature dependence observed after excitation in the B and C high-energy
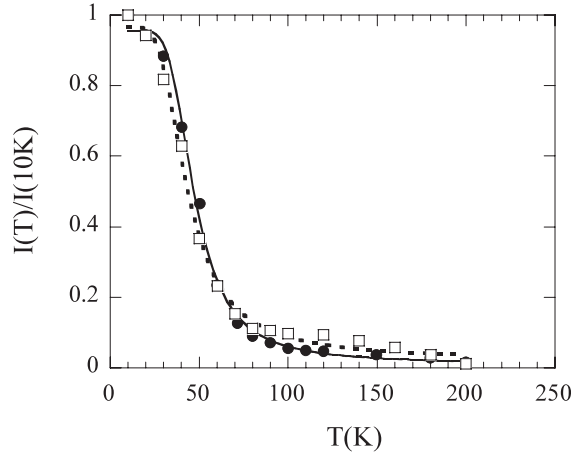
Figure 8. Temperature dependence of the normalized integrated Eu^{2+} PL intensity in CsCdBr$_3$: 0.1% Eu^{2+} after exciting at 4.44 eV (squares) and 4.00 eV (dots). The solid and broken lines represent the fittings to equation (1), where $I_0 = 0.96$, $b = 64$, $E_a = 16$ meV ($E_{exc} = 4.44$ eV), and $I_0 = 0.96$, $b = 178$, $E_a = 21$ meV ($E_{exc} = 4.00$ eV).

absorption bands. We conclude that the emission band centred at 2.53 eV is due to the e$^-$–hole pair recombination, created after excitation at these energies. Within this model, the absorption bands peaking at 4.04 and 4.54 eV would correspond to Rydberg excitonic levels $n = 1$ and 2, respectively, associated with the e$^-$–Eu^{3+} pair in the proximity of the energy gap of the host material. The energy of the excitonic levels can be determined, in the simplest model, from the required energy for inducing an e$^-$–hole pair, E_g, and the binding energy due to the Coulomb interaction, E_b [23]:

$$E_n = E_g - E_b = E_g - \frac{R_X}{n^2}$$

where R_X is the exciton Rydberg constant (related to the effective mass) and E_b can be as great as 1 eV for fluorides, tending to decrease in more polarizable materials such as chlorides or bromides [24]. Below the hypothesis that $E_1 = 4.04$ eV and $E_2 = 4.54$ eV, the binding energy of the e$^-$–Eu^{3+} pair is $E_b = 0.67$ eV (similar to $E_b = 0.7$ eV for KBr), whereas the energy gap $E_g = 4.71$ eV is very close to the value obtained through the absorption spectrum of the pure CsCdBr$_3$ (4.9 eV) [19]. Moreover, the temperature dependence of the emission intensity is attributed to different quenching mechanisms: (i) to a thermal activation of a non-radiative relaxation process resulting from the strong distortion of the excited state with respect to the ground state in a configurational coordinate diagram and (ii) to a thermal excitation from the excitonic levels to the conduction band. Independently of the origin of the intensity quenching, the temperature dependence can be fitted to an Arrhenius model:

$$I(t) = \frac{I_0}{1 + b \cdot e^{-E_a/KT}} \qquad (1)$$

where E_a is the activation energy of the non-radiative process and b is the ratio between the thermal quenching rate, p, $\tau_{NR}^{-1} = p \cdot \exp(-E_a/KT)$, and the inverse of the radiative lifetime, τ_{rad}^{-1} ($b = p/\tau_{rad}^{-1}$). The fitting of the temperature dependence of the PL intensities obtained after 4.44 and 4.00 eV excitation energies is shown in figure 8. The analysis of the experimental data results in $E_a = 16$ and 21 meV for the potential barrier, respectively, and a similar quenching temperature, $T (I_0/2) = 50$ K. These activation energies are similar to the maximum energy

of the lattice phonons of the CsCdBr$_3$ host lattice, $\hbar\omega_{max} = 175$ cm^{-1} [8]. This result points to thermal effects for phonon creation giving rise to the migration of electrons to the conduction band and the eventual recombination as heat emission.

5. Conclusions

The study of the optical properties of Eu^{2+}-doped CsCdBr$_3$ at different concentrations reveals a very complex behaviour, which has not been reported before. We have analysed the origin of the three absorption bands observed in the polarized absorption spectra of CsCdBr$_3$: Eu^{2+}. Two different coupling models can account for the structure of the low-energy band. The high-energy bands have a distinct origin. An impurity self-trapped exciton may be responsible for them. According to this hypothesis we have assigned these bands to excitonic Rydberg levels. The emission after excitation in these bands presents a large Stokes shift and strong temperature dependence due to the recombination between distorted Eu^{2+} levels. The luminescence quenching above 100 K is due to thermal activation of non-radiative processes from a highly distorted excited state with respect to the ground state, or to the jump of the electron to the conduction band.

Acknowledgments

References

[1] McClure D S and Kiss Z 1963 *J. Chem. Phys.* **39** 3251
[2] Loh E 1968 *Phys. Rev.* **175** 533
[3] Rubio J 1991 *J. Phys. Chem. Solids* **52** 101
[4] Takahashi K 2002 *J. Lumin.* **100** 307
[5] Koschnick F K, Spaeth J M, Eachus R S, McDugle W G and Nuttall R H D 1991 *Phys. Rev. Lett.* **67** 3571
[6] Dorenbos P 2003 *J. Lumin.* **104** 239
[7] Dorenbos P 2003 *J. Phys.: Condens. Matter* **15** 2645
[8] Malkin B Z, Iskhakova A I, Kamba S, Heber J, Altwein M and Schaack G 2001 *Phys. Rev.* B **63** 075104
[9] Pellé F, Gardant N, Genotelle M, Goldner P and Porcher P 1995 *J. Phys. Chem. Solids* **56** 1003
[10] Weakliem H A 1972 *Phys. Rev.* B **6** 2743
[11] Duan C K, Reid M F and Burdick G W 2002 *Phys. Rev.* B **66** 155108
[12] Duan C K and Reid M F 2003 *J. Solid State Chem.* **171** 299
[13] Güdel H U 2004 private communication
[14] Meijerink A and Blasse G 1989 *Phys. Rev.* B **40** 7288
[15] Downer M C and Cordero-Montalvo C D 1983 *Phys. Rev.* B **28** 4931
[16] Gamelin D R and Güdel H U 2000 *J. Phys. Chem.* B **104** 10222
[17] Solomon E I and Lever A B P 1999 *Inorganic Electronic Structure and Spectroscopy* (New York: Wiley)
[18] Dorenbos P 2002 *J. Alloys Compounds* **341** 156
[19] Demirbilek R 2002 Spektroskopische untersuchungen am CsCdBr$_3$ *Thesis* Tehnische Universität Darmstadt
[20] Dorenbos P, van Loef E V D, Vink A P, van der Kolk E, van Eijk C W E, Krämer K W, Güdel H U,
     Higgins W M and Shah K S 2006 *J. Lumin.* **117** 147
[21] Wenzel M, Altwein M, Demirbilek R, Leu B, Heber J, Kubler J, Bleeker B and Meijerink A 2000 *J. Alloys
     Compounds* **300** 479
[22] McClure D S and Pedrini C 1985 *Phys. Rev.* B **32** 8465
[23] Fox M 2001 *Optical Properties of Solids* (New York: Oxford University Press)
[24] Song K S and Williams R T 1993 *Self-Trapped Excitons* (Berlin: Springer)